

NUCLEATION AND GROWTH OF THERMAL FATIGUE CRACKS
IN CHEMICALLY UNHOMOGENEOUS TOOL STEEL

L. Kosec, * F. Kosel, ** F. Vodopivec *

The importance of chemical unhomogeneity affecting the phenomenon of heat checking of hot work steel (H 11) is described. The authors treat in detail the characteristics of the geometry and chemical composition of oxide wedges, and the effect of temperature variation as well as oxidation of steel and work metal remains on the appearance and propagation of cracks. By an analytical model the magnitude of stresses on the working surface of plungers from high pressure hot chamber die casting machines, that appeared because of temperature variation and chemical unhomogeneity of steel, has been determined.

INTRODUCTION

Forging tools, casting dies and some parts of die casting machines are subject to thermal loads. On the majority of them there comes to damages in the form of cracks, local fractures, wear, erosion, high temperature corrosion (oxidation) and similar. A very frequent kind of damage of these parts is the so-called heat checking. The phenomenon of heat checking is quite satisfactorily explained in literature (1). The objective of this paper is to call the attention to the influence of the chemical unhomogeneity of steel on the appearance and propagation of cracks in hot work tool steel. The authors have come to the below described results on the basis of an investigation being carried out on plungers from high pressure hot chamber die casting machines for copper alloys.

DESCRIPTION OF EXPERIMENTS

Plungers were made from hot work steel of type H 11 with the following nominal chemical composition (0.4% C, 5.0% Cr, 1.3% Mo and 0.4% V). They were manufactured out of forged bars so that the plunger axis coincided with the axis of the bar. The plunger inside was cooled by water and the steel wall on the working surface was approximately 10 mm thick. The plungers were air quenched from the temperature 1010° C and tempered at the temperature 550° C to have the average hardness about 50 HRC. The working cycle of the machine lasted about 11 sec. so that the plunger was about 4 sec. in contact with the melt and 7 sec. in contact with the air.

* Slovenian Ironworks, Metallurgical Institute, Ljubljana

** Faculty of Mechanical Eng., University Edvard Kardelj in Ljubljana

The surface integrity of the working surface was investigated on axial cross section. The methods of classical metallography and electromicroanalysis were used.

RESULTS

After a certain time of service heat checking develops on the plunger surface which has been in contact with the work metal. The cracks are wide open towards the surface, their edges and/or exits to the surface are rounded, their walls covered with oxide scale. The wide crack channels are on several places more or less filled by the work metal with which the plunger has been in contact. The areas of the oxidized surface between the cracks are corrugated. The frequency of cracks on the surface is higher than shown in the macroscopic image of heat checking, since the exits of numerous cracks are covered by oxide scale. At some places of the plunger surface the final stage of heat checking phenomenon has been observed, i. e. spalling of particular areas in the cracks net.

The steel from which the plungers have been manufactured, has an unhomogeneous chemical composition. The segregation fibres run in the direction of the plunger axis. It has been established that the highest concentrations of chromium in these segregations are about 7% ("positive" segregations), while the lowest concentrations ("negative" segregations) are only about 3%. The molybdenum segregations coincide with those of chromium; the highest concentrations of molybdenum are about 2.5% ... 3%, while the lowest are about 0.5 ... 0.7%, Fig. 1. The segregations of carbon, vanadium and other elements are related to the segregations of these two elements. This chemical unhomogeneity results further in microstructure unhomogeneity and differences in the physico-chemical properties inside steel. This can be assumed from the differences in microhardness measured in the areas with high concentration ("positive" segregation) and in those with under-average concentration of alloying elements. Due to the temperature effect of long duration the hardness on the plunger working surface decreases to the value otherwise possessed by this steel in the "ideal" soft annealed state. The differences in microhardness due to segregations remain practically identical.

On the axial cross section of the plunger cracks have the form of wedges filled by oxide, some of which being at the upper wider part filled also by metal. The wedges are of different forms and depth. The propagation of cracks into the depth is accompanied by simultaneous widening and deepening of the oxide wedge. Some cracks are not visible on the surface because their exits are covered by a continuous oxide layer. At macroscopic surface examination of heat checking these cracks are not seen. The cracks net is much denser than estimated by the one which is seen on the surface. The cracks or wedges having their exits to the surface covered by a layer of oxide are generally shorter than those which are open to the surface. The wedges with several roots have the widest channels on the surface, Fig.

The appearance and propagation of cracks is related to the chemical unhomogeneity of steel. They advance along the channels of "negative" segregations. According to our observations a crack seems to start on the working surface in

the channel of "negative" segregation and propagates along the same channel into the depth. A couple of cases have also been observed where the top of the crack entered the neighbouring negative segregation. If the crack is growing and the oxide wedge widening, it can surpass the steel region and comprises several neighbouring "positive" and "negative" segregations.

The oxide wedge is composed mostly from oxides of iron, zink and chromium, i. e. of the components of steel and work metal. On their edges the oxide wedges are enriched by chromium, silicium and molybdenum. The metal components in craters and cracks in the oxide wedge are practically from pure copper or zink impoverished work metal. Pure copper and zink impoverished work metal appear during a full or partial selective oxidation of the remains of work metal in the oxide wedges. The chemical composition of oxide in one and the same wedge is very unhomogeneous, however still greater are the differences in the quantitative composition of various oxide wedges. In the majority of oxide wedges microscopic cracks and holes have been observed. In the axis of each oxide wedge there generally exists a thin microcrack reaching the wedge top. Thus a fast access of oxygen is possible to the crack or wedge top, (4,5).

The growing of the oxide wedge causes plastic deformation of the steel in its direct neighbourhood. The phenomenon of local plastic deformation can be presumed from the metallographic image of the distribution of segregations. Plastic deformation is the most evident in the wedge neighbourhood near the surface and the wider is the wedge, the longer is the distance in which the steel is deformed. At water cooled plungers cracks propagate over crystall grains, at tools which have not been cooled the propagation of cracks along grain boundaries can also be observed.

INITIATION AND PROPAGATION OF CRACKS

The phenomenon of heat checking is sufficiently explained in literature. However, though the role of external factors such as varying temperature, the effect of oxidation and work metal is clarified, the role of structural and chemical properties of steel is not explained.

In a simplified form chemically unhomogeneous steel is such as if being composed from fibers of different chemical composition. The transitions between the areas of extreme concentrations (fibers) of alloying elements are continuous, and the gradients of the distribution of alloying elements concentration on these transitions are relatively high but they are not equal at all places. The "fibers" (segregations) of steel differ among themselves by physico-chemical properties. In the phenomenon under discussion a very important role is played by the differences in thermal expansion coefficient, heat conductivity, specific heat, mechanical properties and resistance to high temperature corrosion (oxidation), (2,3). The differences in the physical properties inside the chemically unhomogeneous steel result in additional internal stresses, while at the same time in the areas of under-average mechanical and chemical properties cracks will develop and propagate with greater possibility.

In the estimation of stresses caused by the differences in physico-chemical properties due to unhomogeneous steel, we have used data (thermal expansion co-

efficient, heat conductivity, specific heat) for steels of approximately the same average chemical composition as the measured maximal and minimal chromium and molybdenum concentrations in the investigated steel.

CALCULATION MODEL

For the above described case of thermal fatigue cracks a simplified thermo-elastic model has been developed. It has been assumed that the concentrations of alloying elements inside the unhomogeneous steel are distributed according to the sine-law with the period being approximately the same as the average distance between the places with the maximal and minimal concentration of alloying elements l_g . With the chemical composition also the physico-chemical properties are varying.

A section of a semi-plane with domain $D \left\{ \begin{matrix} -1 \leq y \leq ly; \\ 0 \leq z \end{matrix} \right\}$ has been chosen in which lies the layer of the plunger. As assumed the physico-chemical properties are varying in the direction of y-axis. In one working cycle t_1 the temperature on the plunger surface ($z = 0$) varies between the highest T_0 and the lowest T_1 , and as a consequence the temperature field is also a function of time. At the plunger depth ($z = l$) the plunger is cooled by the cooling fluid having the temperature T_e .

Let it be assumed that heat conductivity a in the entire domain D and in the thermal interval $\Delta T = T_0 - T_e$ is approximately equal and constant. In this case from the equation for heat conductivity (6)

$$\frac{\partial^2 T}{\partial z^2} = \frac{1}{a} \frac{\partial T}{\partial t} \dots \dots \dots (1)$$

the temperature field is obtained, taking into account the following boundary and initial conditions:

$$z = 0; T = T_0 f(t); z = l; T = T_e f(t); t = 0; T = \left(\frac{T_e - T_0}{l} z + T_0 \right) f(0) \dots (2)$$

where $f(t)$ is the function determining the time behaviour of the temperature field.

In our case the following time function has been chosen:

$$f(t) = b - ch(gt).$$

The temperature field can then be written as:

$$T(z, t) = b \left(\frac{T_e - T_0}{l} z + T_0 \right) - \frac{T_0 \operatorname{sh}(l-z)\omega + T_e \operatorname{sh}z\omega}{2 \operatorname{sh}l\omega} e^{-gt} - \frac{T_0 \sin(l-z)\omega + T_e \sin z\omega}{2 \sin l\omega} e^{-gt} + \sum_{n=1}^{\infty} f_n(t) \sin \lambda z \dots \dots (3)$$

where: $\lambda = \frac{n\pi}{l}, \quad \omega = \sqrt{\frac{g}{a}}, \quad f_n = \frac{2}{\pi} \frac{T_0 + (-1)^{n-1} T_e}{n \left\{ \left(\frac{\lambda}{\omega} \right)^4 - 1 \right\}} e^{-\left(\frac{\lambda}{\omega} \right)^2 gt}$

The plane stress state can be determined using the Airy's stress function $F = F(y, z, t)$

$$\sigma_y = \frac{\partial^2 F}{\partial z^2} ; \tau_{yz} = \tau_{zy} = -\frac{\partial^2 F}{\partial y \partial z} ; \sigma_z = \frac{\partial^2 F}{\partial y^2} \dots\dots\dots (4)$$

In order to fulfill the requirements of the elasto-mechanical equations and under the assumption that the Young's elasticity module E is constant, the Airy's stress function has to satisfy the following differential equation:

$$\Delta \Delta F + E \Delta(\alpha_t T) = 0 \dots\dots\dots (5)$$

where Δ - Laplace's operator
 α_t - linear thermal expansion coefficient

The plane stress state is determined by taking into account the following boundary conditions

$$z = 0 : \sigma_z = \tau_{zy} = \tau_{yz} = 0 \dots\dots\dots (6)$$

$$\lim_{z \rightarrow \infty} \sigma_{ij} \neq \infty$$

σ_{ij} - stress tensor

and by the requirement that the plunger has to have a prescribed tolerance zone at the working temperature, and therefore the expansion of the plunger in the direction of y -axis is not hindered.

Let it be assumed that the linear thermal coefficient in the direction of y -axis is changing according to the following law, (7):

$$\alpha_t(y) = \alpha_0 + \alpha_1 \sin \alpha y \dots\dots\dots (7)$$

where

$$\alpha = \frac{\pi}{l_s} , \alpha_0 = \frac{1}{2} \{ \alpha_t^{(1)} + \alpha_t^{(2)} \} , \alpha_1 = \frac{1}{2} \{ \alpha_t^{(1)} - \alpha_t^{(2)} \}$$

and

$\alpha_t^{(1)}$ - linear thermal expansion coefficient of the domain with positive segregation

$\alpha_t^{(2)}$ - linear thermal expansion coefficient of the domain with negative segregation

Thus the stresses in domain D of the plunger are:

$$\sigma_y = (-2\alpha D + \alpha^2 C + \alpha^2 D z) e^{-\alpha z} \sin \alpha y - E \omega^2 \alpha_1 \sin \alpha y \cdot \left\{ \frac{T_0 \operatorname{sh}(1-z)\omega + T_e \operatorname{sh} \omega z}{2(\alpha^2 - \omega^2) \operatorname{sh} \omega l} e^{gt} - \frac{T_0 \sin(1-z)\omega + T_e \sin z\omega}{2(\alpha^2 + \omega^2) \sin \omega l} e^{-gt} + \dots \right.$$

$$+ \sum_{n=1}^{n=\infty} f_n \frac{\lambda^2}{\alpha^2 + \lambda^2} \sin \lambda z \}$$

$$\begin{aligned} \tau_{zy} = \tau_{yz} = & (\alpha C - D + \alpha Dz) e^{-\alpha z} \alpha \cos \alpha y + E \alpha \alpha_1 \cos \alpha y \left\{ -\frac{b}{\alpha^2} \right. \\ & \left. \left(\frac{T_e - T_0}{1} \right) + \omega \frac{-T_0 \operatorname{ch}(1-z)\omega + T_e \operatorname{ch} \omega z}{2(\alpha^2 - \omega^2) \operatorname{sh} \omega l} \cdot e^{gt} + \right. \\ & \left. + \omega \frac{-T_0 \cos(1-z)\omega + T_e \cos \omega z}{2(\alpha^2 + \omega^2) \sin \omega l} e^{-gt} - \sum_{n=1}^{n=\infty} \frac{f_n}{\alpha^2 + \lambda^2} \lambda \cos \lambda z \right\} \end{aligned}$$

$$\begin{aligned} \sigma_z = & -\alpha^2 (C + Dz) e^{-\alpha z} \sin \alpha y + E \alpha^2 \alpha_1 \sin \alpha y \left\{ -\frac{b}{\alpha^2} \left(\frac{T_e - T_0}{1} z + \right. \right. \\ & \left. \left. + T_0 \right) + \frac{T_0 \operatorname{sh}(1-z)\omega + T_e \operatorname{sh} \omega z}{2(\alpha^2 - \omega^2) \operatorname{sh} \omega l} e^{gt} + \frac{T_0 \sin(1-z)\omega + T_e \sin \omega z}{2(\alpha^2 + \omega^2) \sin \omega l} e^{-gt} - \right. \\ & \left. - \sum_{n=1}^{n=\infty} \frac{f_n}{\alpha^2 + \lambda^2} \sin \lambda z \right\} \end{aligned} \quad \dots \dots \dots (8)$$

Where

$$\begin{aligned} C = & E \alpha_1 T_0 \left(-\frac{b}{\alpha^2} + \frac{\alpha^2 \operatorname{ch} g + \omega^2 \operatorname{sh} gt}{\alpha^4 - \omega^4} \right) \\ D = & \alpha C - E \alpha_1 \left\{ \frac{b}{\alpha^2} \left(\frac{T_e - T_0}{1} \right) + \frac{T_0 \operatorname{ch} \omega l - T_e}{2(\alpha^2 - \omega^2) \operatorname{sh} \omega l} \omega e^{gt} + \right. \\ & \left. + \frac{T_0 \cos \omega l - T_e}{2(\alpha^2 + \omega^2) \sin \omega l} \omega e^{-gt} + \sum_{n=1}^{n=\infty} \frac{f_n}{\alpha^2 + \lambda^2} \lambda \right\} \end{aligned}$$

For the quantitative analysis which makes possible a comparison of the results of the calculation model to the experimental ones, the following data have been chosen:

| | | |
|---------------------------|--|--|
| $T_0 = 780^\circ\text{C}$ | $E(T_0) = \frac{E(T_e)}{2} = 1,05 \cdot 10^5 \text{ N/mm}^2$ | $a = 8.081 \text{ mm}^2/\text{sec}$ |
| $T_1 = 600^\circ\text{C}$ | $l_y = 26 \text{ mm}$ | $\alpha_t^{(1)} = 14,3 \cdot 10^{-6} \text{ 1/}^\circ\text{C}$ |
| $T_e = 15^\circ\text{C}$ | $b = 2$ | $\alpha_t^{(2)} = 13,1 \cdot 10^{-6} \text{ 1/}^\circ\text{C}$ |
| $l = 10 \text{ mm}$ | $g = 9.528 \cdot 10^{-2} \text{ 1/}^\circ\text{C}$ | $t_1 = 7 \text{ sec}$ |
| $l_s = 0,11 \text{ mm}$ | | |

The stress state functions in dependence upon coordinates y and time t at different depth values can be seen in diagrams, Fig. 4

CONCLUSIONS

The phenomenon of heat checking is affected by internal and external factors. Among the most influential factors belong thermal loads, oxidation and the influence of the melt, while among the most influential internal factors are the chemical and structural unhomogeneity of steel.

Our investigation confirmed that it is thermal fatigue which is the principal reason for the appearance of cracks.

Cracks begin and propagate in the region of "negative" segregations, that is at the place where the steel has the lowest strength and resistance to oxidation.

The propagation of cracks is further influenced also by the oxidation of the steel and the melt as well as by the concentration of the stress due to the continuous effect of the oxide wedge.

The results of the calculation model, Fig. 4 agree with the experimental findings about the effect of the chemical unhomogeneity of steel on the appearance and propagation of cracks.

From the data on steels of corresponding chemical compositions, taken from the catalogue of the Slovenian Ironworks RAVNE, it was estimated that for the area of "positive" segregation the magnitude of tensile strength at temperature $T_0 = 780^\circ\text{C}$ is $\sigma_{zT} = 100\text{N/mm}^2$ and for the area of "negative" segregation $\sigma_{zT} = 80\text{N/mm}^2$.

The stresses determined by the calculation model are tensile in the area of "negative" segregations at $z = 0,25\text{mm}$ and have the magnitude $\sigma_z = 49\text{N/mm}^2$, while σ_x and τ_{xy} can be neglected. With time $t_1 = 7\text{ sec}$ these stresses pulsate for $\Delta\sigma = \pm 6\text{N/mm}^2$.

On the plunger surface ($z = 0$) the stress is $\sigma_y = 49\text{N/mm}^2$ and is compressive at the area of "negative" segregations.

From this we can conclude that the area of "negative" segregations is the place where the appearance of fatigue cracks is the most probable.

REFERENCES

1. B. B. Seth, Review of Heat Checking in Die Casting Dies; Die Casting Eng., Jan., Feb., 1972, 12-36
2. Thermophysical Properties of High Temperature Solid Materials; Vol. 3; Ferrous Alloys; The MacMillan Company, New York, 1967
3. Steel Catalogue, Ironwork Ravne; Metalburo, Zagreb, 1981
4. P. T. Heald, The Oxide Wedging of Surface Cracks, Mater. Sci. and Eng., 35, 1979, 165-169
5. Vlijanje oksidativnih procesov na razvite razgarnih treščin press-form litja pod devleniem; Metalloved. i termič. obrat. metallov, No9, 1980, 51-53
6. Kovalenko A. D. Osnovi termouprugosti, Naukova Dumka, Kiev, 1970
7. Matematičeskie metodi v termomehaniké, Zbornik naučnih trudov, Naukova Dumka, Kiev, 1978

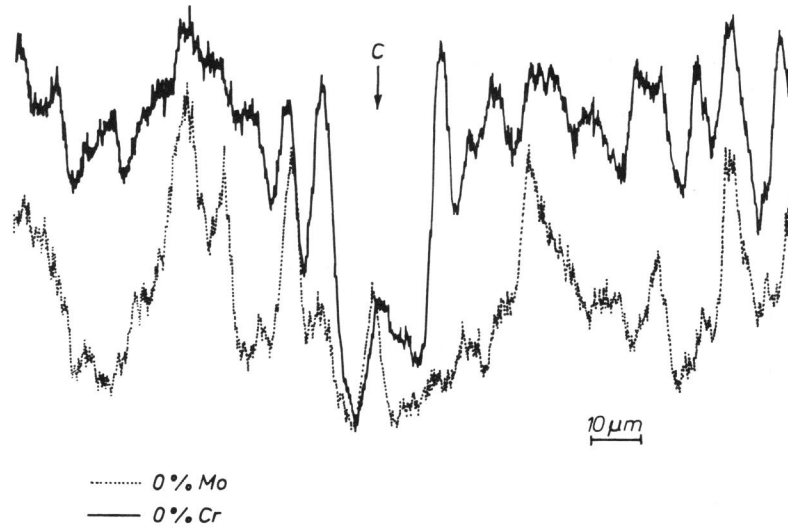


Figure 1 Distribution of chromium and molybdenum in transverse direction to segregation fibers. Arrow C shows the oxide wedge.

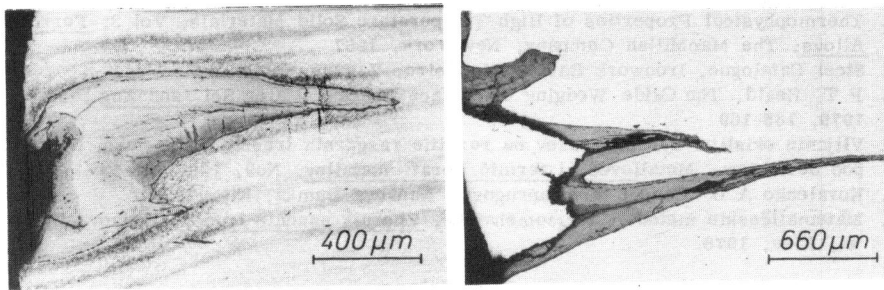


Figure 2 Oxide wedge. White fibers-"negative", dark-"positive" segregations
 Figure 3 Oxide wedge resulting from three cracks; work metal in the wedge (left)

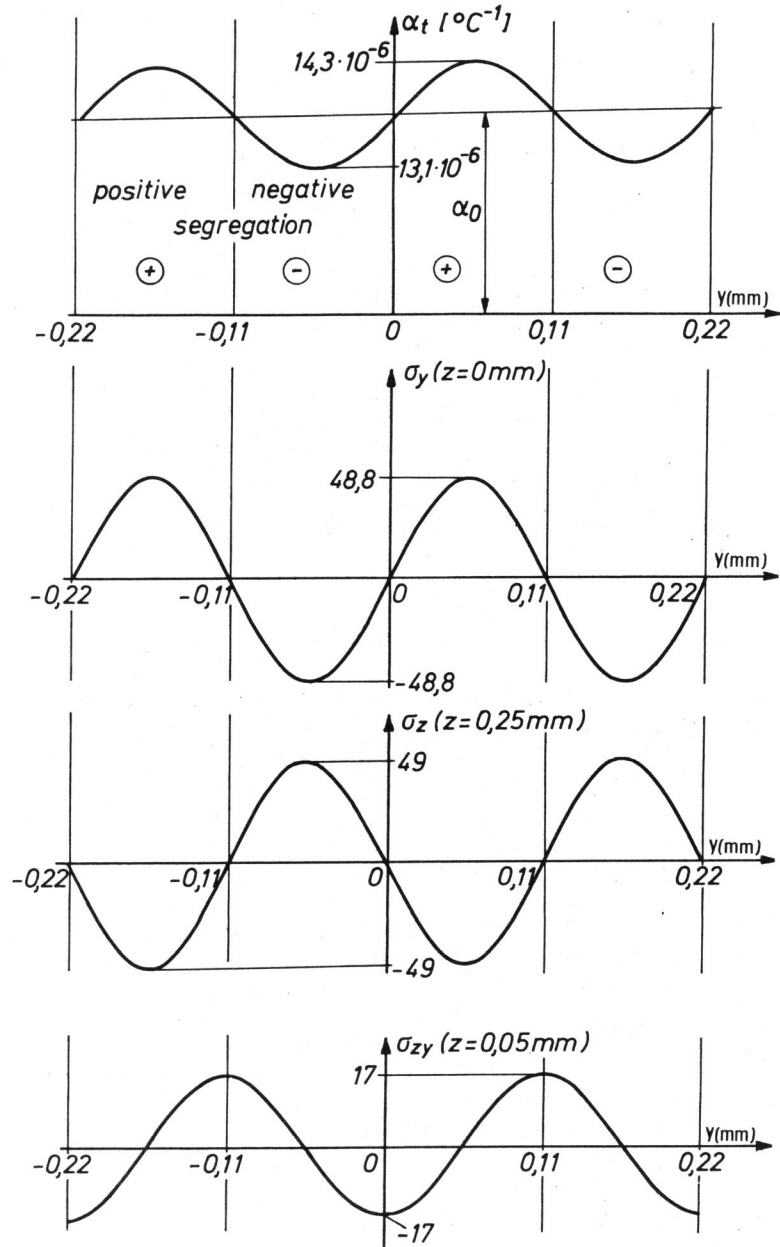


Figure 4 Stress functions σ_y , σ_z , σ_{yz} at different depth values of the plunger related to the areas of "positive" and "negative" segregations in N/mm^2